

Adsorption of Methylene Blue from Aqueous Solution onto Cordierite based Ceramic

D. Njoya^{1*}, J. Ndi Nsami^{2*}, A. Ntieche Rahman³, R. B. Lekene Ngouateu²,
M. Hajjaji⁴, C. Nkoumbou⁵

¹Laboratoire de Physico-Chimie des Matériaux Minéraux, Département de Chimie Inorganique, Faculté des Sciences, Université de Yaoundé I, B.P. 812, Yaoundé, Cameroun.

²Laboratoire de Chimie Physique et Théorique, Département de Chimie Inorganique, Faculté des Sciences, Université de Yaoundé I, B.P. 812, Yaoundé, Cameroun.

³Département de Chimie, Ecole Normale Supérieure, Université de Maroua, B.P.55 Maroua, Cameroun.

⁴Laboratoire de Physico-chimie des Matériaux et Environnement, Unité Associée au CNRST (URAC 20), Département de Chimie, Faculté des Sciences Semlalia, Université Cadi Ayyad, B.P. 2390, Marrakech, Maroc.

⁵Département des Sciences de la Terre, Faculté des Sciences, Université de Yaoundé I, B.P. 812, Yaoundé, Cameroun.

Received 21 Sep2016,
Revised 03 Feb2017,
Accepted 07 Feb 2017

Keywords :

- ✓ Cordierite;
- ✓ Methylene blue;
- ✓ Adsorption;
- ✓ Isotherm Models.

dayirou2000@yahoo.fr;
+237 677 31 35 45;
bigpielo2002@yahoo.com
+237 677 807 132;

Abstract

The adsorption of methylene blue (MB) dye onto synthesized cordierite was investigated. The influence of contact time, pH of dye solution, adsorbent dosage and initial dye concentration on adsorption performances has been examined. The experiments showed that the amount of dye adsorbed increases with increased contact time and attained its equilibrium in 5 minutes. The adsorption capacity reaches its maximum and remains almost constant at pH = 6. Methylene blue adsorption was found to decrease with increasing amount of adsorbent. The amount of dye adsorbed per unit mass of adsorbent increased with increase in MB concentration. The adsorption kinetic obeyed pseudo-second order kinetic model and the best fit isotherm model was Langmuir. In addition, R_L values ranging between 0 and 1 confirmed that the synthesized cordierite is favorable for the adsorption of MB dye from aqueous solution.

1. Introduction

The progressive increase of industrial technology results in the continuous increase in environmental pollution. More than 10,000 of different commercial dyes and pigments exists and about 7×10^5 tones are produced annually worldwide [1]. Industries and farmers discharge these different types of dyes waste into the environment at an unprecedented and at a constant increasing rate. These dye wastes may be discharged into streams, rivers and lakes and the continuous enrichment of these waters with these wastes beyond the healthy level causes poisoning, leading to various sicknesses to human on one hand, and damage to aquatic life on another hand [2].

Dyes are very persistent and are widely used in textile, rubber, paper, plastic, cosmetic industries. [3].The treatment of polluted industrial and farms wastewaters before releasing into the environment remains a topic of global concern. The conventional wastewater treatment, which rely on aerobic biodegradation have low removal efficiency for reactive and other anionic soluble dyes. Due to low biodegradation of dyes, convectional biological treatment processes are not very effective in treating dyes wastewater [4].This implies that, many techniques have been developed for the removal of dyes from aqueous solution, but adsorption technique

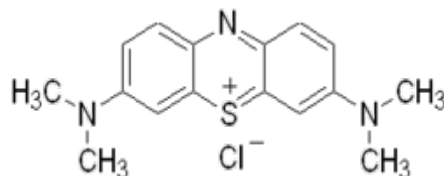
remains the most effective [5]. Methylene blue adsorption by activated carbon, natural and activated clay has been reported [6-12], and due to high cost and low percentage yield of these adsorbents during regeneration, alternative low cost adsorbents have attracted the attention of several investigators to provide an alternate for the high cost activated carbon. However, little attention has been focused on the adsorption of methylene blue by an adsorbent based ceramic product [13, 14].

Thus, the aim of this work was to study the kinetic and equilibrium models of adsorption of methylene blue dye by cordierite synthesized from abundant Cameroonian natural raw materials. The pseudo-first order and pseudo-second order models were used to correlate the adsorption kinetics data of methylene blue dye onto the synthesized cordierite. Equilibrium studies have also been performed to understand the processes of removal of methylene blue dye. Langmuir and Freundlich models are the most frequently employed models. In this work, both models were used to describe the relationship between the amount of MB adsorbed and its equilibrium concentration.

2. Experimental

2.1. Adsorbate

Methylene blue, a cationic dye supplied in powder form by Rieder De Haen, was used without further purification for the preparation of synthetic aqueous solution (100 mg/L) using distilled water. Its molecular formula is $C_{16}H_{18}N_3SCl$ and the structure is:



The chemical formula of methylene blue [12]

Solution of hydrochloric acid (0.1M) and sodium hydroxide (0.1M) was also prepared for pH adjustments.

2.2. Preparation of cordierite (adsorbent)

The basic natural raw materials for the preparation of cordierite were talc (T), kaolinitic clay (MY₃), and bauxite (BX₃). These samples were obtained from three different regions of Cameroon: Boumnyebel; Mayouom; and Minim-Martap. Their chemical and mineralogical compositions are reported in previous studies [15-17]. Two formulations of kaolinitic clay, talc – bauxite mixture were used and are listed in table 1.

The powdered samples were pressed at 30 MPa using few cm³ of water as a binder. Rectangular prisms 50 mm x 10 mm x 6 mm were obtained. The pressed specimens were oven dried at 105 °C to constant weight and fired in an electrical furnace (Nabertherm RHF 1500) at 1300 and 1400 °C [18]. The specimens are placed in the furnace heated at a rate of 5 °C/min up to the desired temperature where they are left for a soaking time of 2h before cooled to room temperature.

Table 1: Mineralogical composition (% wt.) of the mixture

Formulation	Kaolinite	Talc	Bauxite
FO1	50	20	30
FO2	30	40	30

2.3. X-ray diffraction

XRD patterns of sintered products were recorded on a Phillips PW 3040 diffractometer with Cu anode and $K\alpha = 0.15418$ nm. Powdered samples were pressed into pellets so as to oriented the reticular plane of the sample to a particular direction that will respect the Bragg relation using a hydraulic press before XRD measurements

2.4. FT-IR spectroscopy

A Bruker-Vertex 70 spectrometer in the range 4000 - 400 cm^{-1} was used to obtain the FTIR spectra that were used to study the surface chemistry of the adsorbent. The samples were mixed with potassium bromide and the mixtures were pressed into pellets before analysis.

2.5. Batch Adsorption studies

The batch experiments of the adsorption studies were conducted at room temperature (25°C) in a 250 mL screw-cap conical flask. For each run, 0.1–0.5 g of the adsorbent dosage was weighed and placed in the flask containing 20 mL solution of methylene blue of a desired concentration (ranging from 6 to 10 mg /L), pH between 3 and 11. The suspension was stirred for interval of time between 5–30 min using a magnetic agitator and stirrer at a controllable speed. After agitation, the suspensions were filtered using Whatman no. 1 filter paper. The concentration of the filtrate was determined by using a UV-visible spectrophotometer (S23A, Techmel & Techmel USA). The absorbance was measured at the maximum absorption wavelength of 668 nm.

The quantity adsorbed by a unit mass of an adsorbent at equilibrium (Q_e) at an instant, t , was calculated using the relations (1)

$$Q_e = (C_o - C_t/m)V \quad (1)$$

Where C_o is the initial concentration of the adsorbate, Q_e the quantity adsorbed at equilibrium, m the mass of the adsorbent, C_t the concentration at time t and V the volume of the adsorbate.

The kinetics studies were conducted using pseudo-first order and pseudo second order models; for this purpose, $\log(Q_e - Q_t)$ and t/Q_t versus time were plotted. Q_e and Q_t refer to the amounts of dye adsorbed (mg/g) at equilibrium and at each time, t (min), respectively.

3. Results and discussion

3.1. Mineralogical characterization of cordierite (adsorbent)

The XRD patterns of the mixtures fired at different temperatures (figure 1) indicated the presence of cordierite $2\text{MgO} \cdot 2\text{Al}_2\text{O}_3 \cdot 5\text{SiO}_2$ which is the main phase with peaks at 8.45 Å; 4.90 Å; 4.09 Å; 3.39 Å; 3.13 Å and 3.02 Å (PDF 12-303).

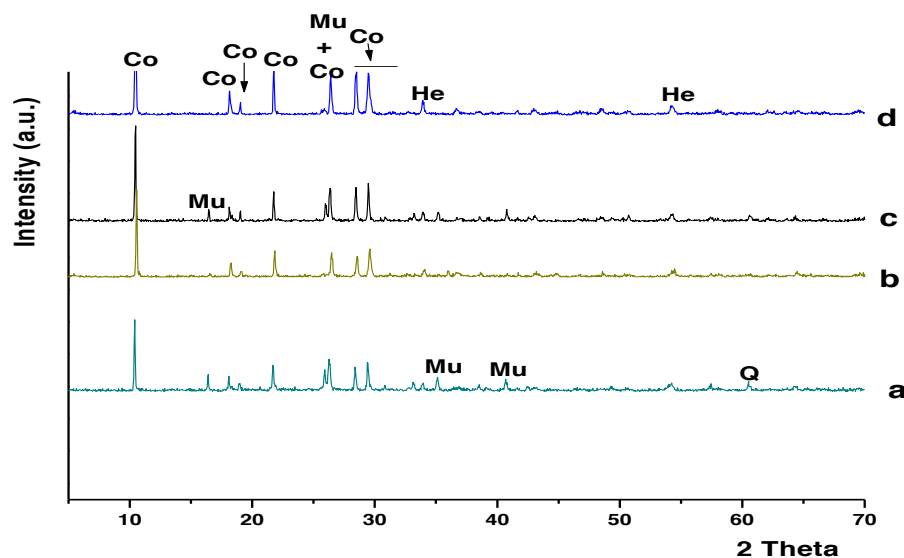


Figure 1: XRD pattern of fired products (Co = cordierite; Mu = mullite; He = hematite; Q = quartz)
(a = FO1, 1300 °C; b = FO2, 1300 °C; c = FO1, 1400 °C; d = FO2, 1400 °C)

Secondary phases include mullite $3\text{Al}_2\text{O}_3 \cdot 2\text{SiO}_2$ with peaks at 5.39 Å; 2.89 Å; 2.55 Å, 1.60 Å (PDF 15-776) and quartz SiO_2 with peaks corresponding to 2.12 and 1.53 Å (PDF 5-490). The hematite Fe_2O_3 was also detected (2.69 Å and 1.69 Å peaks) (PDF 13-534). This hematite peaks are assigned to initial iron oxide contain in the raw material used for the synthesis.

3.2. Fourier Transform Infra-Red spectroscopy

The FTIR spectra are presented in figure 2.

On these FTIR spectra (figure 2), the Mg - O (MgO_6) stretching vibration band was observed at 576 cm^{-1} while the Al - O (AlO_4) stretching vibration band was identified at 955 cm^{-1} and bands at 765 and 1180 cm^{-1} shows Si-O (SiO_4) stretching vibration. The $3200 - 3500\text{ cm}^{-1}$ absorption band is assigned to O-H adsorbed water.

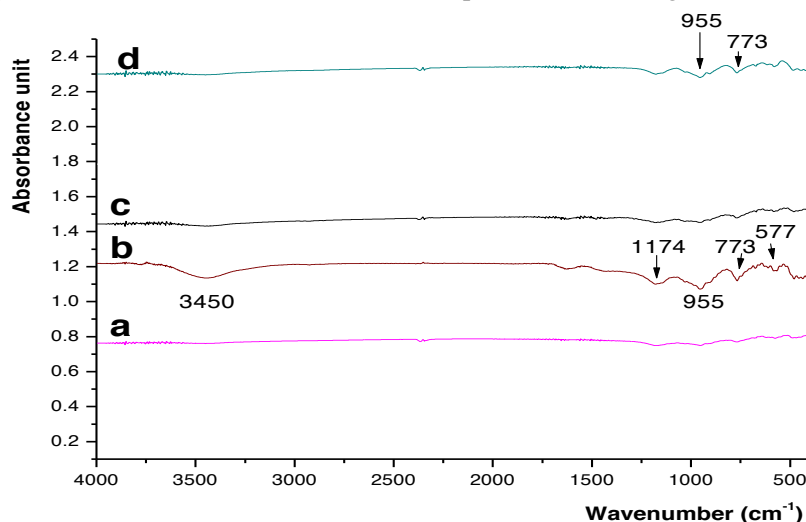


Figure 2: FTIR spectra of fired blends.

(a = FO1, $1300\text{ }^\circ\text{C}$; b = FO2, $1300\text{ }^\circ\text{C}$; c = FO1, $1400\text{ }^\circ\text{C}$; d = FO2, $1400\text{ }^\circ\text{C}$)

3.3. Adsorption contact time test

Adsorption experiments were carried out for different contact time. The results are shown in figure 3. It can be observed that the adsorption rate is very high for the first five minutes. The equilibrium sorption capacity increased rapidly during the first 5 minutes for values of 1.945; 1.998; 1.981 and 1.841 mg/g, respectively, for samples a, b, c and d then decreased slightly and stabilized. This rapid increase is due to the availability of adsorptions sites while the stability of the adsorbed amount over time reflects the almost total occupation of adsorptions sites.

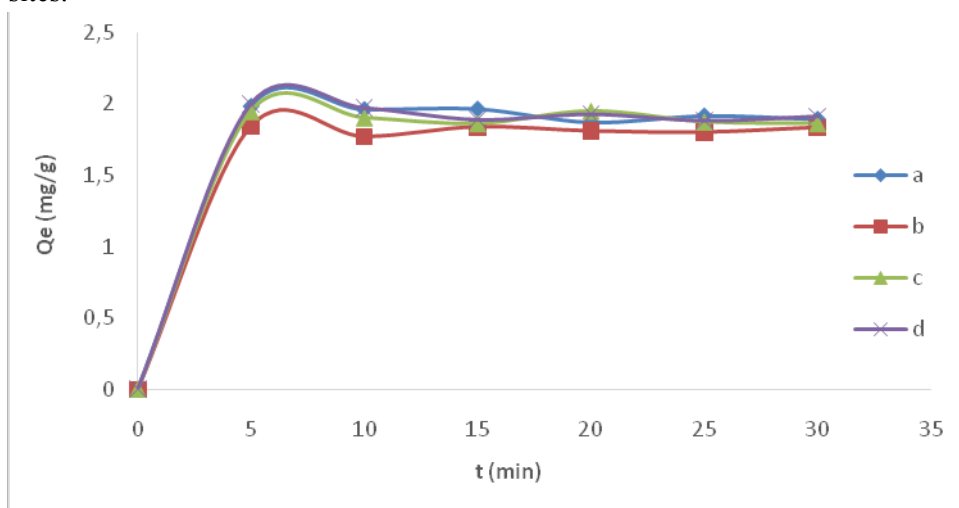


Figure 3: Effect of time on methylene blue adsorption

(a = FO1, $1300\text{ }^\circ\text{C}$; b = FO2, $1300\text{ }^\circ\text{C}$; c = FO1, $1400\text{ }^\circ\text{C}$; d = FO2, $1400\text{ }^\circ\text{C}$)

From figure 2, the structure of the FO2 differ with sintering temperature with the allocation of Si-O(SiO_4) for FO2, $1300\text{ }^\circ\text{C}$ and Al-O(AlO_4) for FO2, $1400\text{ }^\circ\text{C}$. The adsorption of methylene blue using these two structures will favour the silanol group as obtained by LE T. et al. [19]. But FO1 with no surface groups will adsorb

methylene blue due to the mineralogical content which favoured the high temperature transformation of the kaolinite to mullite with more mesopores.

3.4. Effect of pH experiments

The pH of dye solution plays an important role in the whole adsorption process, particularly on adsorption capacity. Figure 4 shows the variation of the amount adsorbed at different pH.

The results showed that adsorption capacity reached the maximum and remained almost constant from pH 6, for a contact time of 10 min where all the sites must have been saturated. This can be explained by the fact that the point of zero charge (PZC) of adsorbents are in the pH range of 3-6 [4]. When $\text{pH} < \text{pH}_{(\text{PZC})}$, adsorbent surfaces are positively charged as those of methylene blue, and the electrostatic repulsion limits the adsorption capacity. When $\text{pH} > \text{pH}_{(\text{PZC})}$, adsorbents surfaces are negatively charged and the electrostatic attraction with methylene blue is very high; thus increase in adsorption capacity [4]. Lower adsorption capacity at acidic pH was also probably due to the presence of excess of H^+ ions competing with the dye cations for adsorption sites. At higher pH value (6 – 12) the dye adsorption was almost constant. The surface of cordierite may contain a large number of active sites, and methylene blue uptake increases as a function of the active sites. Similar trend was observed for adsorption of methylene blue onto yellow passion fruit [20], garlic peel [7]. At $\text{pH} < 5$, adsorption capacity of sample FO1 sintered at 1400°C , is the lowest followed by FO1, 1300°C due to the presence of high mullite content as revealed by XRD (figure 1). The dye adsorption capacity at acid pH seems to be sensitive to mineralogical composition of raw materials (table 1) and firing temperature (figure 1).

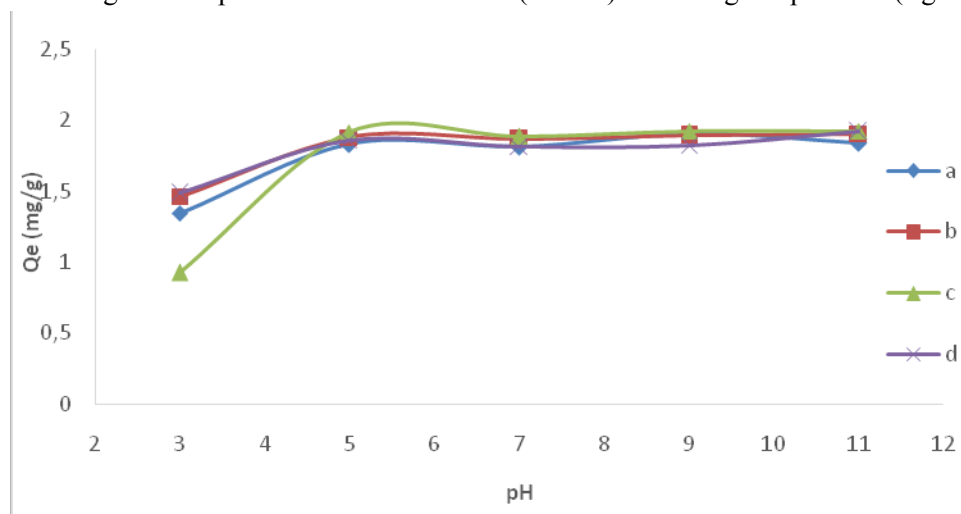


Figure 4: Variation of the amount adsorbed versus pH, at contact time of 10 min. (a = FO1, 1300°C ; b = FO2, 1300°C ; c = FO1, 1400°C ; d = FO2, 1400°C)

3.5. Effect of adsorbent mass

The influence of amount of adsorbent on dye adsorption is shown in figure 5. Dye adsorption was found to decrease with increasing amount of all the adsorbents, mindful of the temperature. For higher adsorbent content, particles agglomerations was formed, leading to adsorption sites reduction, and therefore, reduction in the amount of MB adsorbed per unit mass of adsorbent. Similar results were reported for the adsorption of MB onto activated carbon by Ndi and Ketcha [12] and the adsorption of 2-nitroaniline onto activated carbon by Li et al. [21].

3.6. Influence of initial dye concentration

The adsorption data for the uptake of MB versus initial dye concentration are presented in figure 6. These results indicate that the amount of dye adsorbed per unit mass of adsorbent increased with increase in MB concentration. This is due to increase in the driving force of concentration gradient, as an increase in the initial dye concentration [10, 22].

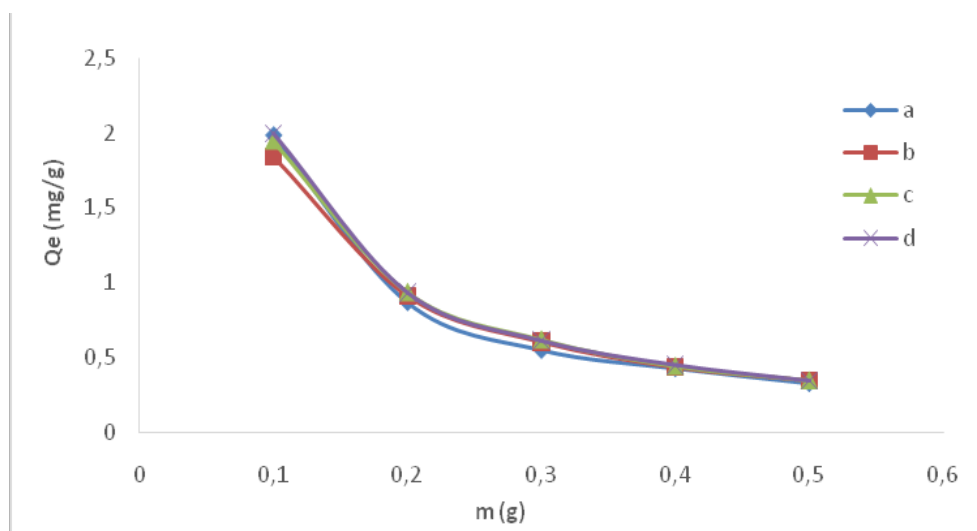


Figure 5: influence of adsorbent content on dye adsorption, at contact time of 10 min. (a = FO1, 1300 °C; b = FO2, 1300°C; c = FO1, 1400°C; d = FO2, 1400 °C)

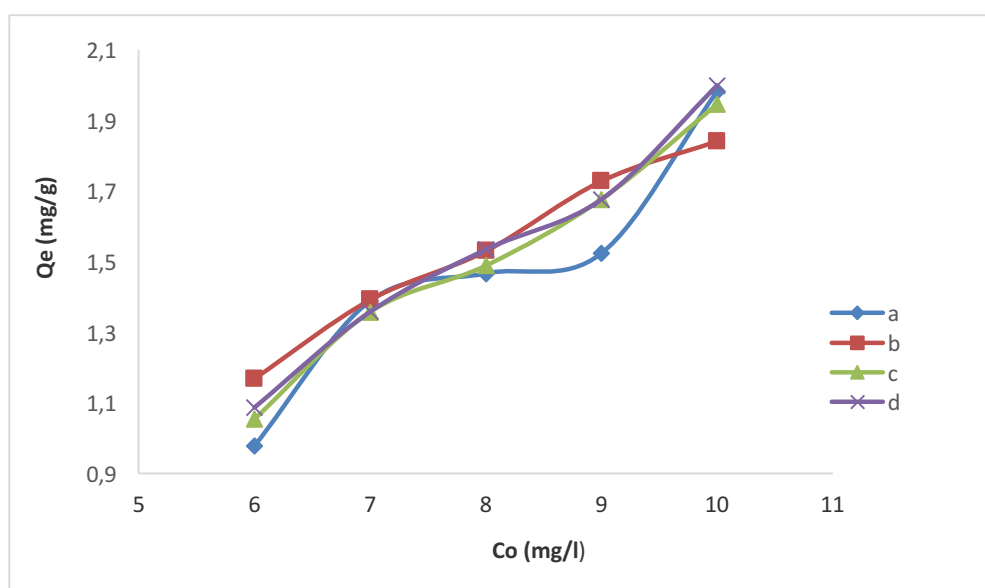


Figure 6: Effect of initial dye concentration on the adsorption of MB, (a = FO1, 1300 °C; b = FO2, 1300°C; c = FO1, 1400°C; d = FO2, 1400 °C)

3.7. Kinetic adsorption models

The pseudo-first- order kinetic model for MB adsorption is represented in figure 7 and the pseudo-second- order in figure 8. The Pseudo-second order model parameters of adsorption of MB onto synthesized cordierite are gathered in table 2.

The curve of $\log(Q_e - Q_t)$ versus time (figure 7) indicates that pseudo-first order model is not appropriated to describe adsorption kinetic of MB on the studied materials due to no correlation of the experimental data. The straight line plot of figure 8 and table 2 data show a good agreement between the pseudo-second order model and the experimental data ($R^2 \geq 0.998$). Moreover, experimental and calculated values (from this model) of Q_e are almost similar (table 2 and figure 3). These results indicate a chemisorption adsorption mechanism. Similar results were reported by Asmaa et al. [6] and HO [23].

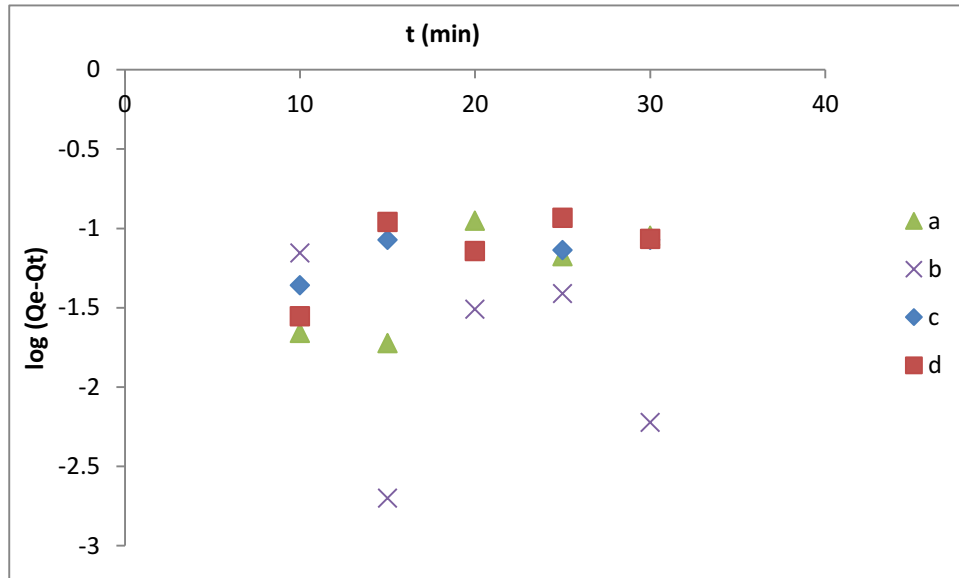


Figure 7: Pseudo-first- order kinetic model for MB adsorption, (a = FO1, 1300 °C; b = FO2, 1300°C; c = FO1, 1400°C; d = FO2, 1400 °C)

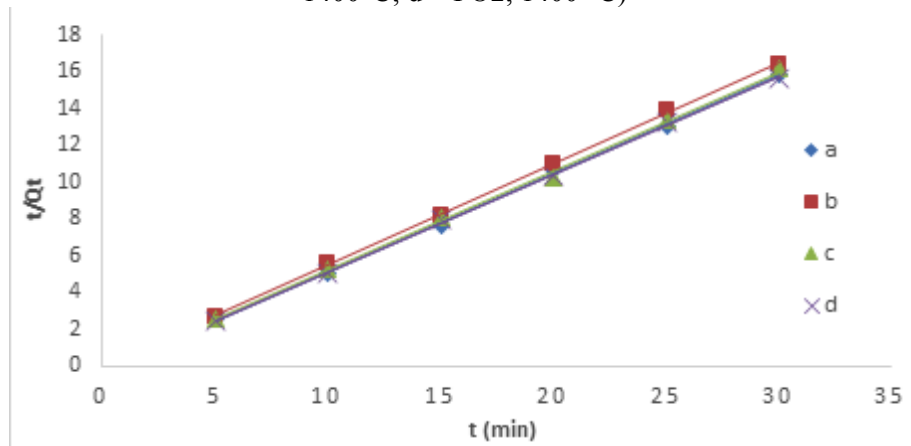


Figure 8: Pseudo-second- order kinetic model for MB adsorption, (a = FO1, 1300 °C; b = FO2, 1300°C; c = FO1, 1400°C; d = FO2, 1400 °C)

Table 2: Pseudo-second order model parameters of adsorption of MB onto synthesized cordierite, (a = FO1, 1300 °C; b = FO2, 1300°C; c = FO1, 1400°C; d = FO2, 1400 °C)

Sample	R ²	K ₂ (g/(mg.min) ⁻¹)	Q _e (mg/g)
a	0,998	1,897	1,856
b	0,999	1,834	1,881
c	0,999	1,345	1,869
d	0,999	5,160	1,828

3.8. Adsorption equilibrium

The adsorption isotherm indicates how the adsorption molecules are being distributed between the liquid phase and the solid phase when the adsorption process reaches equilibrium state. The analysis of the isotherm data by fitting process to different isotherm models is an important step to find the suitable model that can be used for design purpose [10].

3.8.1. Langmuir isotherm

This model is based on certain assumptions: - That each adsorption site can occupy a dye molecule; that the uptake occurs on homogeneous surface by monolayer sorption without interaction between adsorbed molecules; - and that adsorption energy is uniform onto the surface. The Langmuir isotherm is described by the following linear equation:

$$\frac{C_e}{Q_e} = \frac{1}{bQ} + \frac{C_e}{Q} \quad (2)$$

Where Q_e (mg/g) is the amounts of dye adsorbed at equilibrium time, C_e (mg/L) the equilibrium concentration of the adsorbate, Q and b are Langmuir constants related to adsorption capacity and rate of adsorption, respectively. When C_e/Q_e is plotted against C_e , straight line with slope $1/Q$ is obtained (figure 9), indicating that the adsorption of MB on cordierite follows the Langmuir isotherm.

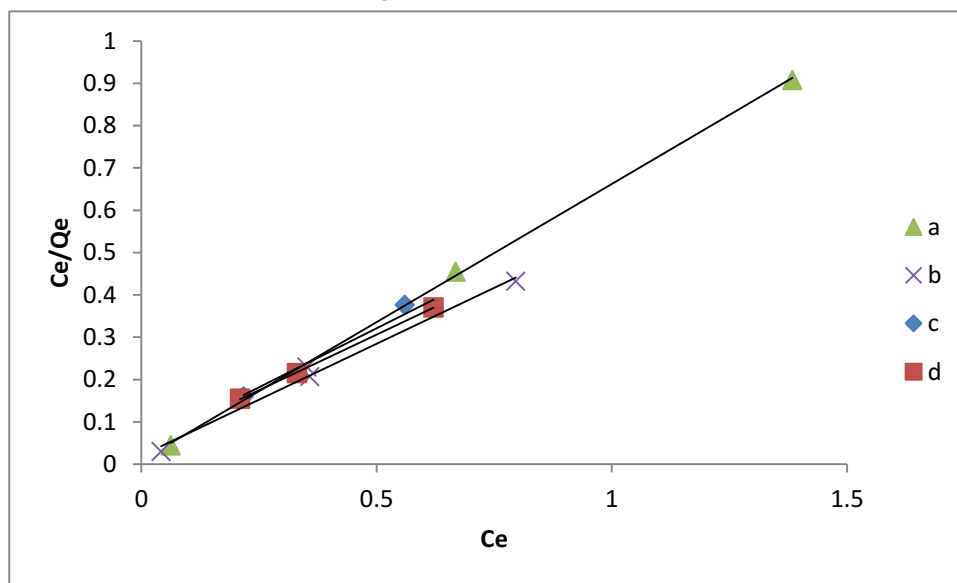


Figure 9: Langmuir adsorption isotherm of MB onto synthesized cordierite, (a = FO1, 1300 °C; b = FO2, 1300°C; c = FO1, 1400°C; d = FO2, 1400 °C)

The Langmuir constants Q and b were calculated from this isotherm and their values are listed in table 3.

Table 3: Langmuir and Freundlich isotherm Parameters, (a = FO1, 1300 °C; b = FO2, 1300°C; c = FO1, 1400°C; d = FO2, 1400 °C)

Isotherm	Paramter	Sample			
		a	b	c	d
Langmuir	R^2	0,9733	0,9999	0,9996	0,9902
	Q (mg/g)	1,7902	1,8983	1,5314	1,8925
	b (L/mg)	13,2999	12,5426	68,0205	25,7389
	R_L	0,0093	0,0099	0,0018	0,0043
Freundlich	R^2	0,7638	0,9666	0,9625	0,8017
	$1/n$	0,1596	0,1908	0,0282	0,0886
	K_F (mg/g)(L/mg) ^{1/n}	1,7227	1,8526	1,4976	1,8212

The results demonstrate the formation of monolayer coverage of dye molecule at the outer surface of the adsorbent. Similar observations were reported by the adsorption of MB onto activated carbon prepared from rattan sawdust [24] and the adsorption of nickel (II) ions by smectite clay [25].

The essential characteristic of Langmuir isotherm can be expressed by a dimensionless constant called separation factor, R_L represented by the following equation [25]:

$$R_L = \frac{1}{1 + bC_0} \quad (3)$$

where b is the Langmuir constant and C_0 (mg/L) the highest initial MB concentration. The value of R_L indicates the type of the isotherm.

According to R_L values, the adsorption is favorable for $0 < R_L < 1$; linear unfavorable for $R_L > 1$; and irreversible for $R_L = 0$. R_L values range between 0 and 1 (table 3), which indicate favorable adsorption of MB dye onto cordierite under the conditions of the present study.

3.8.2. Freundlich isotherm

The Freundlich model is appropriate for the description of multilayer adsorption with interaction between adsorbed molecules [17]. This isotherm is described by the following linear equation:

$$\ln Q_e = \ln K_F + \frac{1}{n} \ln C_e \quad (4)$$

Where Q_e (mg/g) is the amounts of dye adsorbed at equilibrium time, C_e (mg/L) the equilibrium concentration of the adsorbate. K_F and n are Freundlich constants; $1/n$ is the heterogeneous factor and K_F the adsorption capacity of the adsorbent.

The Freundlich Isotherm for MB adsorption on the synthesized cordierite is represented in figure 10 and the Langmuir and Freundlich isotherm Parameters are gathered in table 3. Figure 10 shows a straight line with a slope of $1/n$ ranging between 0 and 1 (table 3). Values of $1/n$ below 1 indicate the heterogeneous surface of the adsorbent and Langmuir isotherm [24].

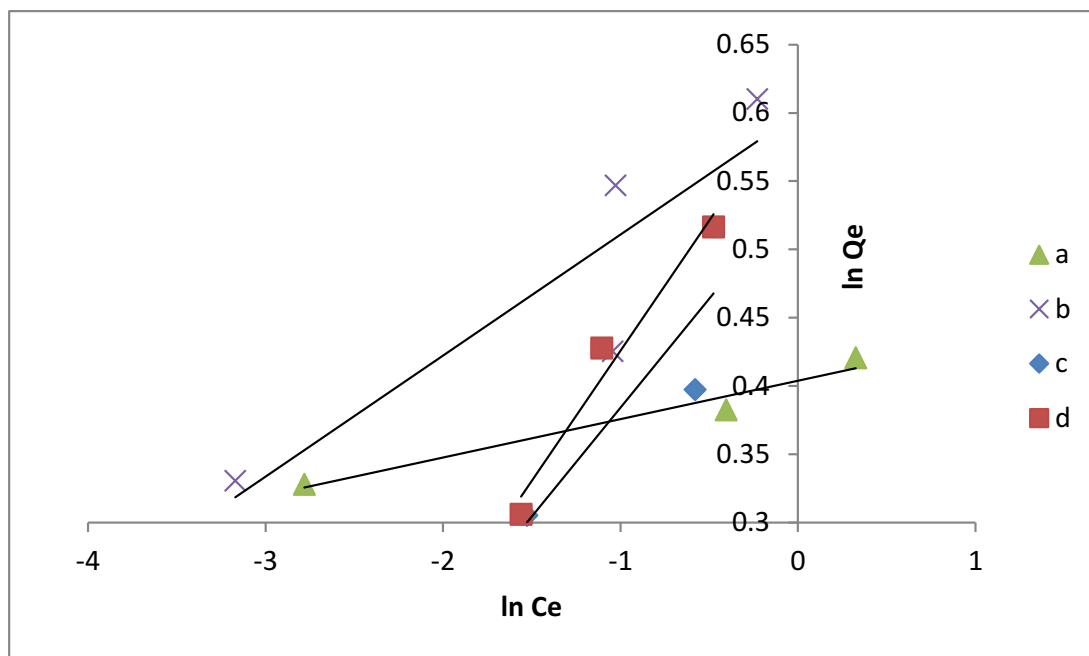


Figure 10: Freundlich Isotherm for MB adsorption by synthesized cordierite, (a = FO1, 1300 °C; b = FO2, 1300°C; c = FO1, 1400°C; d = FO2, 1400 °C)

Conclusion

The aim of this work was to study the kinetic and equilibrium models of adsorption of methylene blue dye by cordierite synthesized from abundant Cameroonian natural raw materials. The synthesized cordierite has been found as a potential adsorbent for MB from aqueous solutions. This adsorption has been well described by Pseudo-second order kinetic model according to the correlation coefficient (R^2) values that range from 0.9733 to 0.9999. Also, experimental and calculated values of Q_e (give the respective value) from this model are almost similar.

The straight line plot of C_e/Q_e versus C_e indicates that the adsorption of MB on cordierite follows the Langmuir isotherm. In addition, R_L value ranging between 0 and 1 indicates that the adsorption of MB dye is favorable on the synthesized cordierite.

Acknowledgements-The authors wish to thank Professor KETCHA Joseph MBADCAM, head of the Physical and Theoretical Chemistry Laboratory, University of Yaoundé I, for the provision he made with some of the laboratory equipment,

References

1. Timi T., Erepanowei Y., Diepreye E. Sch., *Acad. J. Biosci.* 2 (2014) 607.
 2. Ketcha J. M., Anagho S. G., Ndi J.N., Maguie A. K., *J. Environ.Chem. Ecotox.* 3 (2011) 290.
 3. Tan I. A. W., Hameed B. H., Ahmad A. L., *Chem. Eng. J.* 127 (2007) 111.
 4. Sachin M., Kanawade, Gaikwad R. W., *Int. J. Chem. Eng. Appl.* 2 (2011) 317.
 5. Robinson T., McMullan G., Marchant R., Nigam P., *Bioresour. Technol.* 77 (2001) 247.
 6. Asmaa K. B., Badia M., Hachkar M., Bakasse M., Yaacoubi A., *J. water Sci.* 23 (2010) 375.
 7. Hajjaji M., Alam A., El Bouadili A., *J. Hazard. Mater.* 135 (2006)188.
 8. Hajjaji M., Alami A., *Appl. Clay Sci.* 44 (2009) 127.
 9. Hajjaji M., El Arfaoui H., *Appl. Clay Sci.* 46 (2009) 418.
 10. Hameed B. H., Ahmed A. L., Latiff, K. N. A., *Dyes and pigments* 75 (2007) 143.
 11. Jiawei S., Younan X., Yan Z., *Appl. Clay Sci.* 46 (2009) 422.
 12. Ndi J. N., Ketcha, J. M., *J. Chem.* (2013) 1.
 13. Nirjan D., Susan J., Jagadeesh B., *Int. J. Adv. Res. Chem. Sci.* 3 (2016) 1.
 14. Fangwen LI., Xiaoai W.U., Songjiang M.A., Zhongjian X.U., Wenhua LI.U., Fen LI.U., *J. Water Res. Prot.* 1 (2009) 1
 15. Njoya D., Elimbi A., Nkoumbou C., Njoya A., Njopwouo D., Lecomte G., Yvon J., *Ann. Chim. Sci. Mat.* 32 (2007) 55.
 16. Nkoumbou C., Njoya A., Njoya D., Grosbois C., Njopwouo D., Coutin –Nomade A., Yvon J., Martin F. , *Appl. Clay Sci.* 43 (2009) 118.
 17. Tchamba A. B., Yongue R., Chinje M. U., Kamseu E., Njoya D., Njopwouo D., *Sil. Ind.* 73 (2008) 77.
 18. Bin T., YouWei F., ShuRen Z., HaiYan N., ChunYu J. *Indian J. Eng. Mater. Sci.* 18 (2011) 221.
 19. Le T. S., Naoto M. and Teruo H., *Clay Sci.* 10, (1998) 315.
 20. Pavan F. A., Mazzocato A. C., Gushikem Y., *Bioresour. Technol.* 99 (2008) 3162.
 21. Li K., Zheng Z., Huang X., Zhao G., Feng J., Zhang J., *J. Hazard. Mater.* 166 (2009) 213.
 22. Gürses A., Doğar Ç., Yalçın M., Açıkıldiz M., Bayrak R. R., Karaca S. , *J. Hazard. Mater.* 131 (2006) 217.
 23. Ho Y. S., *J. Hazard. Mater.* 136 (2006) 681.
 24. Hameed B. H., Hamad A. A., *J. Hazard. Mater.* 164 (2009) 870.
 25. Ketcha J. M., Dongmo S., Dinka'a N. D., *Int. J. Curr. Res.* 4 (2012) 162.
-